



## LJMU Research Online

Gao, R, Ji, Z, Zhang, JF, Zhang, WD, Hatta, SFWM, Niblock, J, Bachmayr, P, Stauffer, L, Wright, K and Greer, S

**A Discharge-Based Pulse Technique for Probing the Energy Distribution of Positive Charges in Gate Dielectric**

<http://researchonline.ljmu.ac.uk/2143/>

### Article

**Citation** (please note it is advisable to refer to the publisher's version if you intend to cite from this work)

**Gao, R, Ji, Z, Zhang, JF, Zhang, WD, Hatta, SFWM, Niblock, J, Bachmayr, P, Stauffer, L, Wright, K and Greer, S (2015) A Discharge-Based Pulse Technique for Probing the Energy Distribution of Positive Charges in Gate Dielectric. IEEE TRANSACTIONS ON SEMICONDUCTOR MANUFACTURING.**

LJMU has developed **LJMU Research Online** for users to access the research output of the University more effectively. Copyright © and Moral Rights for the papers on this site are retained by the individual authors and/or other copyright owners. Users may download and/or print one copy of any article(s) in LJMU Research Online to facilitate their private study or for non-commercial research. You may not engage in further distribution of the material or use it for any profit-making activities or any commercial gain.

The version presented here may differ from the published version or from the version of the record. Please see the repository URL above for details on accessing the published version and note that access may require a subscription.

For more information please contact [researchonline@ljmu.ac.uk](mailto:researchonline@ljmu.ac.uk)

<http://researchonline.ljmu.ac.uk/>

# A discharge-based pulse technique for probing the energy distribution of positive charges in gate dielectric

R. Gao, Z. Ji, Member, IEEE, J. F. Zhang, W. D. Zhang, S. F. Wan Muhamad Hatta, J. Niblock, P. Bachmayr, L. Stauffer, K. Wright and S. Greer

**Abstract**— Characterizing positive charges and its energy distribution in gate dielectric is useful for process qualification. A discharge-based technique is introduced to extract their energy distribution both within and beyond substrate band-gap. This work investigates the difficulties in its implementation on typical industrial parameter analyzer and provides solutions. For the first time, we demonstrate the technique's applicability to the advanced 22 nm fabrication process and its capability in evaluating the impact of different strains on the energy distribution. The test time is within several hours. This, together with its implementation on industrial parameter analyzer, makes it a useful tool in the semiconductor manufacturing foundries for process monitoring and optimization.

**Keywords**— Energy distributions, energy profiles, positive charges, hole traps, negative bias temperature instability (NBTI).

## I. INTRODUCTION

Negative Bias Temperature Instability (NBTI) has been identified as a major reliability issue for pMOS devices. It is well-known that both positive charges (PCs) formation within the gate dielectric and the generation of interface states contribute to the long-term degradation [1-4]. PCs shift important parameters, such as threshold voltage [5] and mobility [6], eventually shortening the transistor lifetime and causing circuit failure [7]. To simulate the impact on circuit performance, the energy distribution of PCs is required. Conventionally, the charge pumping (CP) technique [8-10] is a widely used method for probing PCs' energy distribution. However, it can only probe traps within the Si band gap. A modern pMOSFET typically operates with the Fermi-level at the interface below the top edge of the valence band, where the CP cannot probe. The Charge Injection and Sensing (CIS) technique proposed recently [11] requires no new trap generation and all the traps being charged and discharged repeatedly. However, these conditions cannot be met for PCs in pMOSFETs.

Manuscript received MMM DDD, 2014. This work was supported by the Engineering and Physical Science Research Council of UK. The review of this paper was arranged by Editor W. WWW.

R. Gao, Z. Ji, J. F. Zhang and W. Zhang are with the School of Engineering, John Moores University, Liverpool L3 3AF, U.K. (e-mail: z.ji@ljmu.ac.uk).

S. F. Wan Muhamad Hatta is with Department of Electrical Engineering, University of Malaya, Malaysia.

J. Niblock, P. Bachmayr, L. Stauffer, K. Wright and S. Greer are with Keithley, Cleveland, Ohio, 44139, USA.

An energy profiling technique is introduced, enabling probing the energy distribution of positive charges both within and beyond band gap, based on the customized test facilities [12]. In this work, we investigate the difficulties in implementing it on a typical industrial parameter analyzer, the Keithley's 4200-SCS analyser with 4225 pulse IV modules, and provide solutions. To demonstrate it as a robust tool for material and process optimization, the energy distributions of PCs are compared for processes with and without strains. It also provides the charge density for a given surface potential required by device modelling.

## II. DEVICES

pMOSFETs with 22nm planar fabrication process are used in this work to demonstrate the applicability of the technique to advanced CMOS nodes. The dielectric stack of the samples is HfO<sub>2</sub> with an Al<sub>2</sub>O<sub>3</sub> cap layer. The gate is TiN. To demonstrate the capability of this technique in evaluating different processes and materials, two pMOSFETs fabricated with and without applying compressive strain in the channel are used for comparison. Unless specified, the channel length and width of the device used is 1  $\mu\text{m}$  and 10  $\mu\text{m}$ , respectively.

## III. DISTRIBUTION EXTRACTION TECHNIQUE

### A. Principle and procedure for energy distribution extraction

The principle of the discharge-based technique [13] for positive charge (PC) energy distribution extraction is shown in Fig. 1.

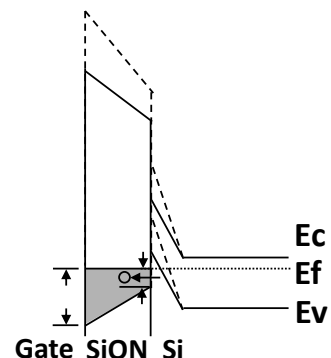


Fig 1: The energy diagram to show the principle for the new discharge-based technique

Firstly, a high negative bias was applied on a pMOSFET (i.e. the sample is with the n-type substrate) for PC formation. Then  $|V_g|$  will be lowered by a small step,  $\Delta V$ , to  $|V_g - \Delta V|$ . Some of the charged PC will fall below Fermi level,  $E_f$ , as marked by the grey shade in Fig.1. As a first order approximation [12, 14-16], below  $E_f$ , positive charges are assumed to be neutralized throughout the oxide, if a sufficient discharge time is given. When  $V_{\text{discharge}}$  moves further towards positive for each step,  $\Delta V$ , the energy level of positive charges is lowered against the substrate, bringing a new shaded region below  $E_f$  for discharging.

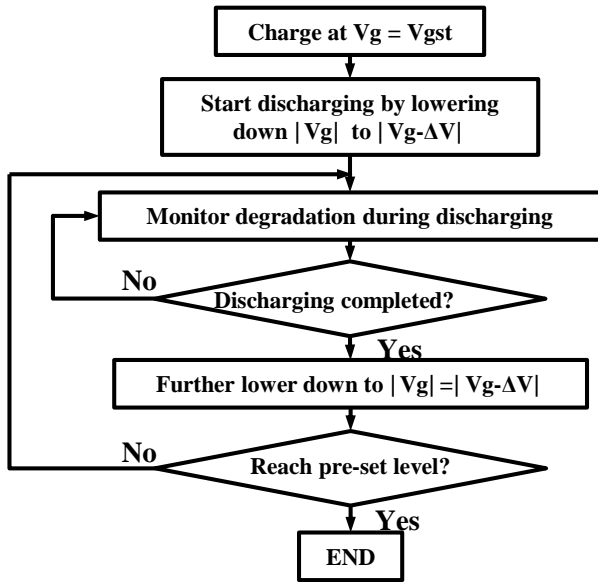


Fig 2 Flowchart of the test procedure.

By varying  $V_{\text{discharge}}$  over a sufficiently large range, one can sweep  $E_f$  over a wide energy range at the interface, including the region beyond  $E_c$  and  $E_v$  of silicon.

The flowchart and the typical  $V_g$  waveforms are given in Fig. 2 and Fig. 3. The device was firstly stressed at  $V_g = V_{\text{gst}}$  for a pre-specified time. Fig. 3 shows that  $|V_g|$  was then lowered to  $|V_{\text{discharge},1}|$ . The degradation, is evaluated by measuring current,  $I_d$ , under a constant sensing voltage,  $V_{g,m}$ . Its conversion to  $\Delta V_t$  will be introduced in Section B. Degradation can be evaluated against discharge time until its change becomes negligible (e.g.  $\Delta V_t < 3\text{mV}$ ). After completing discharge at  $|V_{\text{discharge},1}|$ ,  $|V_g|$  was further reduced to  $|V_{\text{discharge},2}|$  and the same procedure is followed. To capture a wide energy range,  $V_{\text{discharge}}$  eventually becomes more positive than the  $V_{g,m}$  for the sensing current level. The direction of pulse will be reversed then, as illustrated.

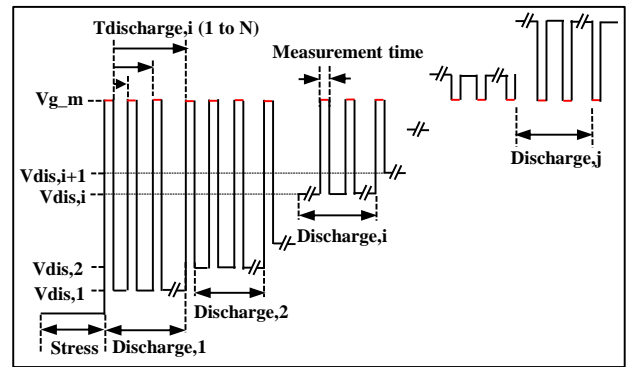


Fig 3  $V_g$  waveforms for the proposed discharge-based energy profiling technique

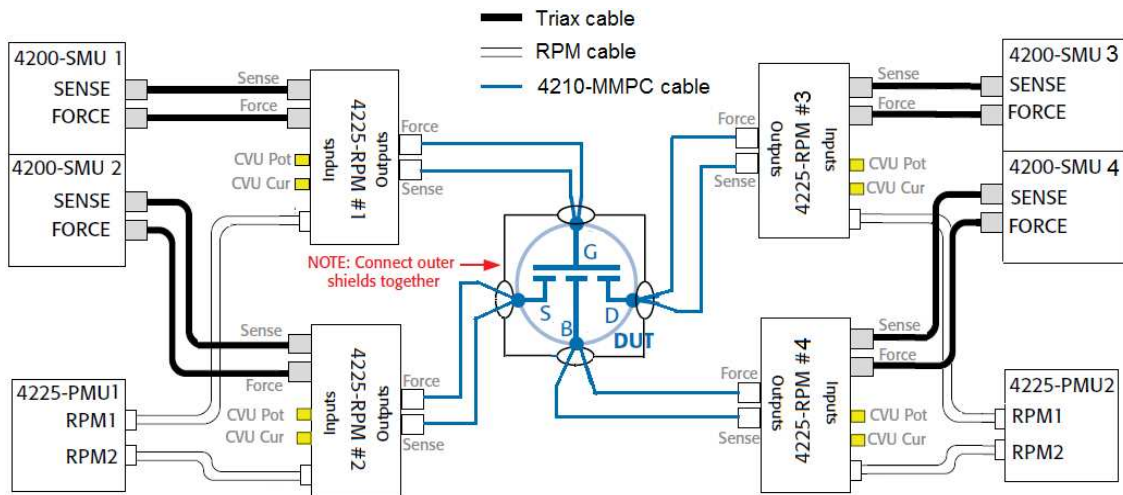


Fig 4: Experimental setup for the proposed technique. Two Keithley dual-channel 4225-PMUs are used for transient measurements. Four Keithley 4225-RPMs are used to reduce cable capacitance effect and to achieve accurate measurement below 100 nA.

## B. Characterization methodology with commercial test equipment

To make the technique a useful tool for semiconductor foundries in material and process qualification, the technique should be implemented on commercial

equipment. In this section, we use Keithley 4200-SCS system as an example, which is one of the mainstream semiconductor testing equipment available in the market. In order to monitor degradation during discharging period, two requirements must be met: 1) the measurement must be fast enough to assure there is no further discharging during the

measurement. 2) The  $V_{th}$  measured under different discharging levels must correspond to the same surface potential.

The first requirement can be met by using the fast measurement capability provided by 4200-SCS system with transient Current-Voltage measurement setup [17], as shown in Fig. 4. Two Keithley dual-channel 4225-PMUs were used for performing transient measurements and four Keithley 4225-RPMs were used to reduce cable capacitance effect and achieve accurate measurement below 100 nA within several  $\mu$ s. The impact of measurement speed is checked and shown in Fig. 5. After stressing the device for 1 ks, the degradation is monitored with different sweep speeds. When measurement speed is slow, clear recovery can be observed. However, when the measurement time is kept shorter than 20  $\mu$ s [3, 12], the recovery becomes negligible.

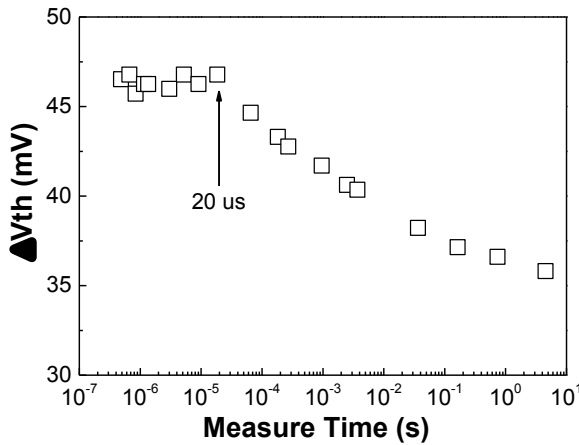


**Fig 5** Measurement time effect on monitoring the degradation. When measurement time increases, the monitored degradation becomes smaller due to the well-known recovery. However, when the measurement time is kept shorter than 20  $\mu$ s, the degradation is fully captured.

Conventionally, the second requirement is met by measuring the entire  $I_d \sim V_g$  and then extracting  $V_t$  by using either the constant current method [12, 18] or the max-gm extrapolation method [19]. This is supported by typical instruments for the standard Stress-Measure-Stress (SMS) sequence. However, if transient Current-Voltage measurement setup is applied, due to the limitation of maximum available data storage provided by the mainstream commercial equipment, only a limited number of  $I_d \sim V_g$  curves can be saved in the memory (at most 15 curves). To overcome this difficulty, we propose using a constant voltage method [20]: degradation is monitored by only measuring a single  $I_d$  current under a certain sensing  $V_{g,m}$ . By measuring under a constant  $V_{g,m}$ , a change of positive charges in the gate dielectric will change the substrate surface potential, so that the positive charges are actually measured at different surface potential during charging or discharging process.

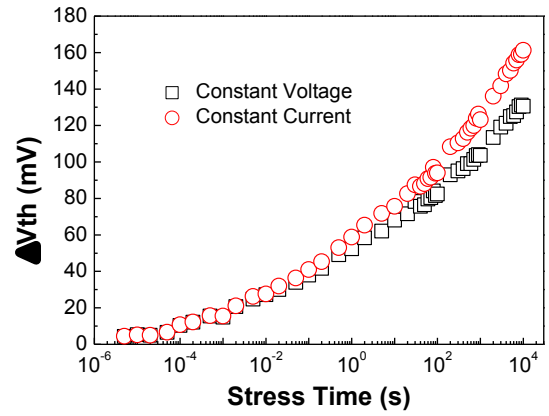


**Fig 6** The impact of different sensing techniques on the degradation. The increase of  $\Delta V_{th}$  will reduce the surface potential if the constant sensing  $V_g$  is used and thus leads to the lower degradation when compared with sensing at the constant current level which is approximately at the same surface potential.

As can be seen in Fig. 6, if the degradation is small ( $<30$ mV),  $\Delta V_{th}$  from two methods (constant current v.s. constant voltage) are comparable. However, when  $\Delta V_{th}$  further increases, degradation from constant voltage method becomes lower than constant current method. This is because high  $\Delta V_t$  lower the Fermi level if  $V_g$  is kept as a constant.

We propose a solution to enable the conversion between measured  $\Delta I_d$  under  $V_{g,m}$  and  $\Delta V_t$  sensed under the same surface potential. The device is firstly stressed under typical NBTI conditions. A series of full  $I_d \sim V_g$  curves were measured where both the  $\Delta V_t$  from a constant current extrapolation and the  $\Delta I_d/I_{d0}$  at a constant sensing  $V_{g,m}$  were extracted. Fig. 7 shows that the relation between them is independent of stress conditions and can be fitted by a cubic equation. Once this unique relation is established, it can be used to convert the  $\Delta I_d/I_{d0}$  measured under a constant  $V_{g,m}$  with the procedure described in section A to  $\Delta V_t$ .

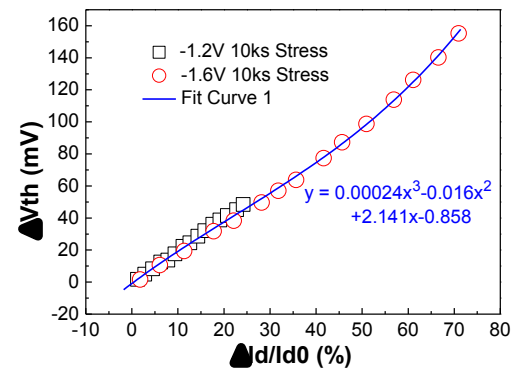


**Fig 7** Experimental extracted unique relationship between  $\Delta I_d/I_{d0}$  and  $\Delta V_{th}$ . Wherein,  $\Delta I_d/I_{d0}$  is taken from the constant sensing  $V_{g,m}$  and the  $\Delta V_{th}$  is from constant current method. This relationship is independent of stress condition and can be used to perform the conversion.

To demonstrate the applicability of this technique to advanced CMOS nodes, it is applied to one pMOS

fabricated by a 22 nm process. The typical result is shown in Fig. 8. Under each  $V_{\text{discharge}}$ , the discharging process completes quickly after about 20s.

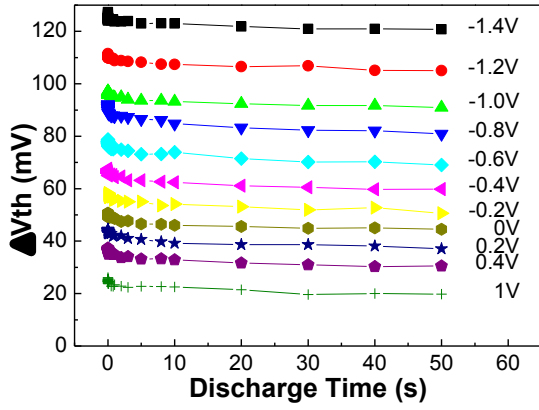


Fig 8: Typical results for discharging under different  $V_{\text{discharge}}$ . The discharge time is the time under a given  $V_{\text{discharge}}$  as marked in Fig. 3. The device is stressed at -1.6 V for 10 ks before the discharging.

### C. Extraction of energy distribution

The proposed technique assumes  $\Delta N_{\text{ox}}$  are the PCs above  $E_f(V_{\text{discharge}})$ . However, in principle, the PCs above  $E_f(V_{\text{discharge}})$  also have small possibility to discharge. Its impact can be assessed by comparing the energy distribution extracted from different discharge time. The  $\Delta V_t$  obtained from discharge time of 10s, 50s and 100s under each  $V_{\text{discharge}}$  in Fig.8 is converted to effective charge density [21, 22], i.e.  $\Delta N_{\text{ox}} = |\Delta V_t| \times C_{\text{ox}}/q$ , and plotted against  $V_{\text{discharge}}$  in Fig. 9(a). The extracted energy distribution overlap each other indicating the impact is negligible.

To obtain the energy distribution,  $V_{\text{discharge}}$  must be converted to the energy level  $E_f$  relative to  $E_v$ , i.e.  $E_f - E_v$ . As shown by the inset of Fig. 9(c),  $E_f - E_v = E_g/2 + \Phi_B - \Phi_S$ . A theoretical  $(E_f - E_v) \sim V_g$  curve is first calculated using the CVC simulator [23]. By shifting the theoretical curve towards left until  $E_f - E_v = E_g/2 - \Phi_B$  (i.e. the strong inversion condition) occurs at the measured  $V_t$ , the  $E_f - E_v$  versus  $V_{\text{discharge}}$  were obtained and used to convert  $V_{\text{discharge}}$  into  $E_f - E_v$ . Fig. 10(a) plots  $\Delta N_{\text{ox}}$  against  $E_f - E_v$ . By differentiating  $\Delta N_{\text{ox}}$  against  $E_f - E_v$ , the energy density,  $\Delta D_{\text{ox}}$ , was obtained as shown in Fig. 10(b).

The impact of generated interface states,  $\Delta N_{\text{it}}$ , has not been taken into account in the analysis above.  $\Delta N_{\text{it}}$  can affect the analysis in two ways: 1)  $\Delta N_{\text{it}}$  contributes to  $\Delta N_{\text{ox}}$  measured at the sensing  $I_d$ ; 2)  $\Delta N_{\text{it}}$  causes a distortion of  $(E_f - E_v) \sim V_g$  curve. The effect of  $\Delta N_{\text{it}}$  has been corrected and a comparison is made before and after correction in Fig.9(a) & Fig.10(a) [12]. The contribution of  $\Delta N_{\text{it}}$  to  $\Delta N_{\text{ox}}$  is modest and its impact on  $\Delta N_{\text{ox}}$  is insignificant under our test conditions.

A closer observation of Fig. 10(a) indicates that PCs behave differently in different energy regions. When  $E_f - E_v$  is swept towards positive,  $\Delta N_{\text{ox}}$  declines quickly initially, leading to a high energy density,  $\Delta D_{\text{ox}}$ . The declining of  $\Delta N_{\text{ox}}$  slows down around  $E_f - E_v = 0.1$  eV, giving a smaller

$\Delta D_{\text{ox}}$ . Fig. 10 shows that this technique can probe the energy distribution of PCs both within and beyond the band gap for advanced CMOS nodes.

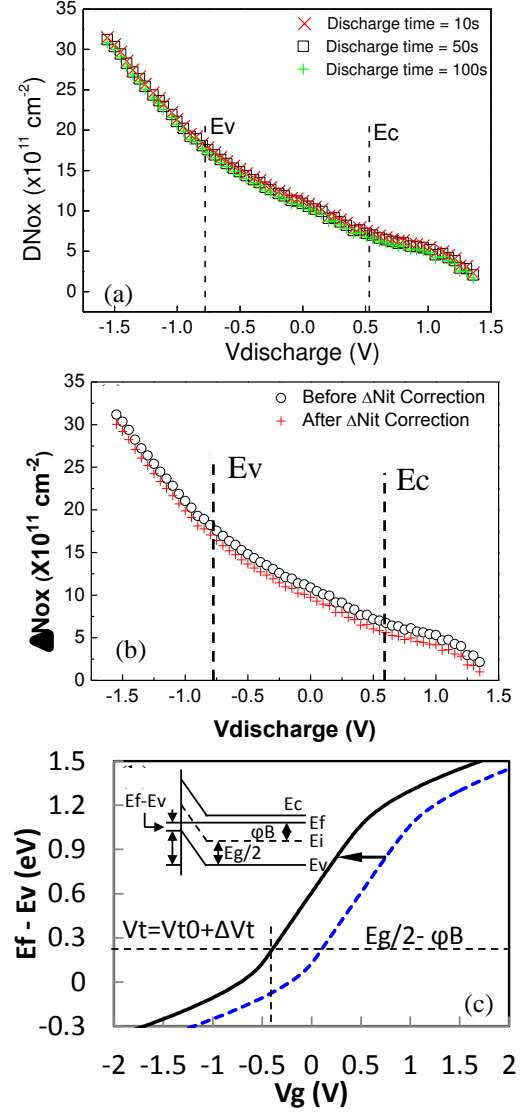


Fig 9: (a) shows the PCs after completing discharging at each  $V_{\text{discharge}}$ , i.e.  $\Delta N_{\text{ox}}$ , converted from  $\Delta V_t$  at different discharge time. (b) shows the comparison before and after Nit correction. (c) shows the conversion between  $E_f - E_v$  and  $V_{\text{discharge}}$ . The dashed curve is the theoretical  $(E_f - E_v) \sim V_g$ , calculated from the CVC simulator. By aligning  $E_f - E_v = E_g/2 - \Phi_B$  to the threshold voltage of stressed device, the solid line is obtained with which  $E_f - E_v$  can be found for a given  $V_g = V_{\text{discharge}}$ . The inset of (c) shows the relationship between  $E_f - E_v$  and surface potential,  $\Phi_s$  and,  $\Phi_B$ .

### IV MATERIAL AND PROCESS EVALUATION WITH DEFECT ENERGY DISTRIBUTION

The ever evolving advanced sub-micron technologies result in the complex and varying materials and processes for the gate stacks. This energy probing technique can evaluate the impact of different fabrication processes on PCs distribution. As an example, the impact of strain on the degradation and PC energy distribution is studied here. Two

pMOSFETs are used, one without and the other with strain along the channel direction.

The typical NBTI results of these two samples are shown in Figure 11(a). The degradation is compared under the same stress field. The result shows that strain enhances the device degradation, agreeing with the literature [24]. In order to find out where this enhancement comes from, the developed energy profiling technique is applied and the effective charge density,  $\Delta N_{ox}$  and its corresponding energy density,  $\Delta D_{ox}$ , against  $E_f - E_v$  is shown in Fig. 11(b) and (c) respectively. Clearly, the PCs can be separated into two regions. Region I is below  $E_v$  where  $E_f - E_v$  is negative.  $\Delta N_{ox}$  against  $E_f - E_v$  are in parallel, leading to the same energy density of the PCs in this region. However, for Region II when  $E_f - E_v$  is positive (i.e. above  $E_v$ ),  $\Delta N_{ox}$  and  $\Delta D_{ox}$  are larger for the strained pMOSFET. The substantial strain-enhanced aging in Figs. 11(a) & (b) originates from PCs above  $E_v$ , therefore. Early works [25, 26] reported that the PCs are from as-grown hole traps below  $E_v$  and from the generated defects above  $E_v$ . This work supports this framework by showing, for the first time, that the as-grown hole traps are insensitive to strain, whilst the strain enhances trap generation.

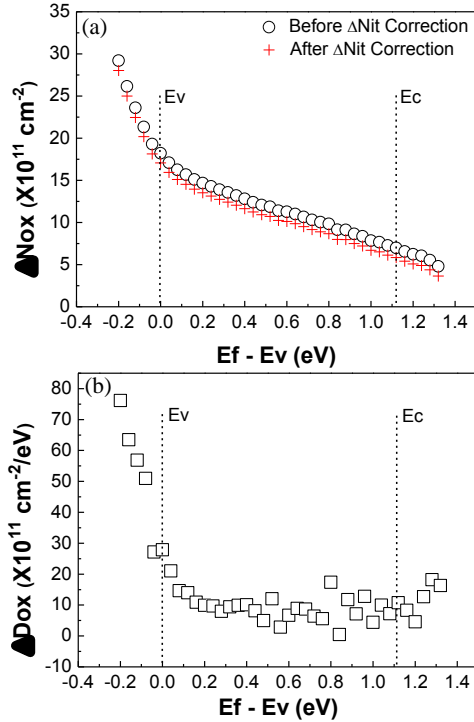


Fig 10: (a) The  $\Delta N_{ox}$  is plotted against  $E_f - E_v$ . The symbol '+' denotes the data after  $\Delta N_{it}$  contribution is corrected. The  $\Delta D_{ox}$  in (b) is the energy density of PCs, obtained by differentiating the data in (a): To extract  $\Delta D_{ox}$  at  $E_f(i)$ , the differentiation is calculated by using two neighboring points  $i+1$  and  $i-1$  through the equation  $\Delta D_{ox}(i) = (\Delta N_{ox}(E_f(i+1) - E_v) - \Delta N_{ox}(E_f(i-1) - E_v)) / (E_f(i+1) - E_f(i-1))$ .

#### IV. CONCLUSION

Discharge-based pulse technique for probing the energy distribution of positive charges in the gate dielectric is

developed based on a typical industrial parameter analyser, after finding a solution to overcome the difficulties. Its applicability to the advanced CMOS nodes has been demonstrated. It was then used to study the impact of strain on the NBTI aging. For the first time, we report that the strain-enhanced aging originates from the generated defects above the  $\text{Si } E_v$ , whilst the as-grown hole traps below  $E_v$  are not affected by the strain. The test takes several hours, acceptable for a typical foundry. This makes it a useful tool for process monitoring and optimization. The technique also allows evaluation of effective PCs for a given surface potential, one key information needed for device and circuit modelling.

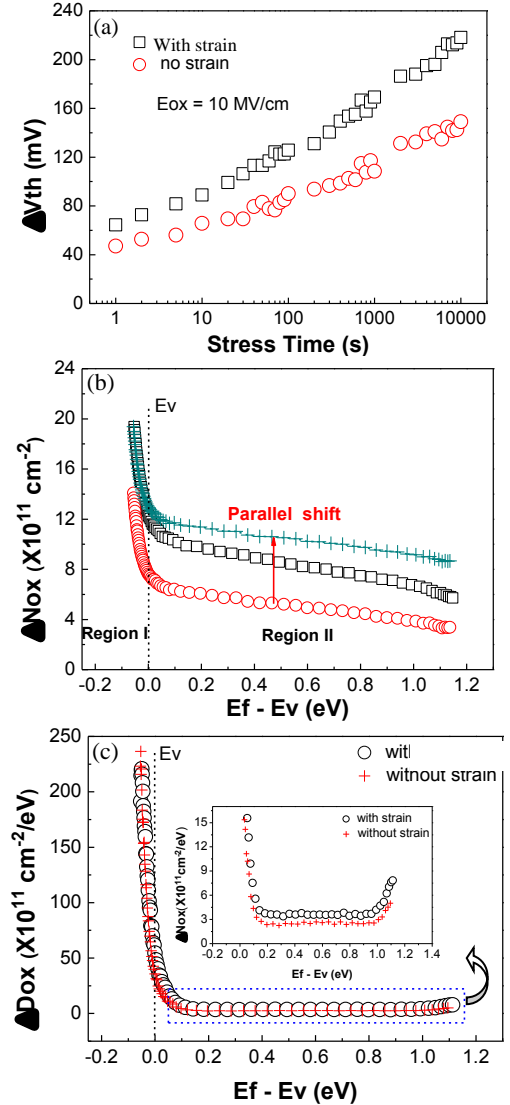


Fig. 11 (a) Typical NBTI stress test on the unstrained and strained pMOSFET. The same electric field is applied during the stress which is 10 MV/cm. (b) PCs energy profiling comparison for the two devices. The  $\Delta N_{ox}$  is plotted against  $E_f - E_v$ , which is converted from  $V_{discharge}$  by applying the proposed procedure explained in Fig. 9(b). (c) The PC energy density,  $\Delta D_{ox}$ , is plotted against  $E_f - E_v$ .

## Acknowledgments

The authors would like to thank B. Kaczer and G. Groeseneken of IMEC, Belgium, for supply of test samples used in this work. This work was supported by the Engineering and Physical Science Research Council (EPSRC) of UK under the grant no. EP/L010607/1.

## REFERENCES

- [1] T. Grasser, B. Kaczer, W. Goes et al., "The paradigm shift in understanding the bias temperature instability: from reaction-diffusion to switching oxide traps," *IEEE Transactions on Electron Devices*, vol. 58, no. 11, pp. 3652-3666, 2011.
- [2] J. Zhang, "Defects and instabilities in Hf-dielectric/SiON stacks," *Microelectronic Engineering*, vol. 86, no. 7, pp. 1883-1887, 2009.
- [3] Z. Ji, J. F. Zhang, M. H. Chang et al., "An analysis of the NBTI-induced threshold voltage shift evaluated by different techniques," *IEEE Transactions on Electron Devices*, vol. 56, no. 5, pp. 1086-1093, 2009.
- [4] Z. Ji, L. Lin, J. F. Zhang et al., "NBTI lifetime prediction and kinetics at operation bias based on ultrafast pulse measurement," *IEEE Transactions on Electron Devices*, vol. 57, no. 1, pp. 228-237, 2010.
- [5] D. K. Schroder, and J. A. Babcock, "Negative bias temperature instability: Road to cross in deep submicron silicon semiconductor manufacturing," *Journal of Applied Physics*, vol. 94, no. 1, pp. 1-18, 2003.
- [6] T. Hori, "Inversion layer mobility under high normal field in nitrided-oxide MOSFETs," *IEEE Transactions on Electron Devices*, vol. 37, no. 9, pp. 2058-2069, 1990.
- [7] M. Agarwal, B. C. Paul, M. Zhang et al., "Circuit failure prediction and its application to transistor aging," in *VLSI Test Symposium, 2007. 25th IEEE 2007*, pp. 277-286.
- [8] G. Groeseneken, H. E. Maes, N. Beltran et al., "A reliable approach to charge-pumping measurements in MOS transistors," *IEEE transactions on Electron Devices*, vol. 31, no. 1, pp. 42-53, 1984.
- [9] W. Zhang, J. Zhang, M. Uren et al., "On the interface states generated under different stress conditions," *Applied Physics Letters*, vol. 79, no. 19, pp. 3092-3094, 2001.
- [10] L. Lin, Z. Ji, J. F. Zhang et al., "A single pulse charge pumping technique for fast measurements of interface states," *IEEE Transactions on Electron Devices*, vol. 58, no. 5, pp. 1490-1498, 2011.
- [11] R. Degraeve, M. Cho, B. Govoreanu et al., "Trap spectroscopy by charge injection and sensing (TSCIS): A quantitative electrical technique for studying defects in dielectric stacks," in *IEEE International Electron Devices Meeting(IEDM)*, 2008, pp. 1-4.
- [12] S. W. M. Hatta, Z. Ji, J. F. Zhang et al., "Energy distribution of positive charges in gate dielectric: Probing technique and impacts of different defects," *IEEE Transactions on Electron Devices*, vol. 60, no. 5, pp. 1745-1753, 2013.
- [13] Z. Ji, S. M. Hatta, J. F. Zhang et al., "A new technique for probing the energy distribution of positive charges in gate dielectric," in *IEEE International Conference on Microelectronics Test Structures (ICMTS)*, 2014.
- [14] T. Aichinger, M. Nelhiebel, S. Einspieler et al., "Observing two stage recovery of gate oxide damage created under negative bias temperature stress," *Journal of Applied Physics*, vol. 107, no. 2, pp. 024508, 2010.
- [15] X. Ji, Y. Liao, F. Yan et al., "The energy distribution of NBTI-induced hole traps in the Si band gap in PNO pMOSFETs," in *IEEE International Reliability Physics Symposium (IRPS)*, 2012, pp. XT. 12.1-XT. 12.5.
- [16] Z. Ji, S. F. W. M. Hatta, J. F. Zhang et al., "Negative bias temperature instability lifetime prediction: Problems and solutions," in *IEEE International Electron Devices Meeting(IEDM)*, 2013, pp. 15.6.1-15.6.4.
- [17] Z. Ji, J. Gillbert, J. Zhang et al., "A new Ultra-Fast Single Pulse technique (UFSP) for channel effective mobility evaluation in MOSFETs," in *IEEE International Conference on Microelectronics Test Structures (ICMTS)*, 2013, pp. 64-69.
- [18] Z. Teo, D. Ang, and C. Ng, "Separation of hole trapping and interface-state generation by ultrafast measurement on dynamic negative-bias temperature instability," *IEEE Electron Device Letters*, vol. 31, no. 7, pp. 656-658, 2010.
- [19] A. Ortiz-Conde, F. Garcia Sánchez, J. J. Liou et al., "A review of recent MOSFET threshold voltage extraction methods," *Microelectronics Reliability*, vol. 42, no. 4, pp. 583-596, 2002.
- [20] J. Zhang, Z. Ji, M. Chang et al., "Real  $V_{th}$  instability of pMOSFETs under practical operation conditions," in *IEEE International Electron Devices Meeting(IEDM)*, 2007, pp. 817-820.
- [21] M. Chang, and J. Zhang, "On positive charge formed under negative bias temperature stress," *Journal of Applied Physics*, vol. 101, no. 2, pp. 024516, 2007.
- [22] C. Zhao, and J. Zhang, "Effects of hydrogen on positive charges in gate oxides," *Journal of applied physics*, vol. 97, no. 7, pp. 073703, 2005.
- [23] J. Hauser, and K. Ahmed, "Characterization of ultra-thin oxides using electrical CV and IV measurements," in *International conference on characterization and metrology for ULSI technology 1998*, pp. 235-239.
- [24] B. Liu, P. S. Y. Lim, and Y.-C. Yeo, "Effect of strain on Negative Bias Temperature Instability of Germanium p-channel Field-Effect Transistor with high- $\kappa$  gate dielectric," in *IEEE International Reliability Physics Symposium (IRPS)*, 2010, pp. 1055-1057.
- [25] J. F. Zhang, M. H. Chang, and G. Groeseneken, "Effects of Measurement Temperature on NBTI," *IEEE Electron Device Letters*, vol. 28, no. 4, pp. 298-300, 2007.
- [26] C. Z. Zhao, J. F. Zhang, C. Mo Huai et al., "Stress-Induced Positive Charge in Hf-Based Gate Dielectrics: Impact on Device Performance and a Framework for the Defect," *IEEE Transactions on Electron Devices*, vol. 55, no. 7, pp. 1647-1656, 2008.